

Electric field effect on short-range polar orders in a relaxor ferroelectric system

Zhijun Xu,^{1,2} Fei Li,^{3,4} Shujun Zhang,⁵ Christopher Stock,⁶ Jun Luo,⁷ Peter M. Gehring,¹ and Guangyong Xu¹

¹NIST Center for Neutron Research, National Institute of Standards and Technology, Gaithersburg, Maryland 20877, USA

²Department of Materials Science and Engineering, University of Maryland, College Park, Maryland, 20742, USA

³Department of Materials Science and Engineering, Materials Research Institute, Pennsylvania State University, University Park, Pennsylvania 16802, USA

⁴Electronic Materials Research Laboratory, Key Laboratory of the Ministry of Education and International Center for Dielectric Research, Xian Jiaotong University, Xian 710049, China

⁵Institute for Superconducting and Electronic Materials, Australian Institute of Innovative Materials, University of Wollongong, Wollongong, New South Wales 2500, Australia

⁶School of Physics and Astronomy, University of Edinburgh, Edinburgh EH9 3JZ, United Kingdom

⁷TRS Technologies Inc., 2820 E College Avenue, State College, PA 16801

Short-range polar orders in the relaxor ferroelectric material $\text{PbMg}_{1/3}\text{Nb}_{2/3}\text{O}_3$ -28% PbTiO_3 (PMN-28PT) have been studied using neutron diffuse scattering. An external electric field along [110] direction can affect the diffuse scattering in the low temperature rhombohedral/monoclinic phase. Diffuse scattering intensities associated with [110] short-range polarizations are partially suppressed, while those arising from [1 $\bar{1}$ 0] polarizations are enhanced. On the other hand, short-range polar orders along other equivalent $\langle 110 \rangle$ directions, *i.e.* [101], [10 $\bar{1}$], [011], and [01 $\bar{1}$] directions, are virtually unaffected by the field. Our results, combined with previous work, strongly suggest that most part of short-range polar orders in PMN-*x*PT relaxor systems are robust in the low temperature phase, where they couple strongly to ferroelectric polarizations of the surrounding ferroelectric domains, and would only respond to an external field indirectly through ferroelectric domain rotation.

PACS numbers: 63.20.kk, 75.30.Ds, 75.85.+t, 75.25.-j, 61.05.fg

$\text{PbMg}_{1/3}\text{Nb}_{2/3}\text{O}_3$ (PMN) is a prototypical lead based relaxor system where no long-range polar order can be established without an external electric field¹⁻⁴. Due to the existence of strong random field⁵⁻⁹, short-range polar orders (SRPO), or, sometimes referred to as "polar nano-regions" (PNR) start to appear in the system at the Burns temperature $T_d \sim 620$ K and grow with cooling¹⁰. These SRPO are believed to contribute to many unique properties of the relaxor material¹¹. When mixed with the classical ferroelectric PbTiO_3 (PT), spontaneous ferroelectric polarizations can start to develop, and the solid solutions of PMN-*x*PT naturally exhibit combined ferroelectric and relaxor characteristics. In the mean time, the system shows extraordinary piezoelectric properties when approaching the Morphotropic Phase Boundary (MPB). There is evidence that the SRPO are important for the high piezoelectric responses as well¹²⁻¹⁴. The relaxor properties gradually disappear when the system crosses MPB into the regime of classic ferroelectrics¹⁵⁻¹⁸. For those with low PT concentrations, *i.e.* on the left side of the MPB, the SRPO can actually persist into the low temperature long-range ferroelectric ordered phase^{19,20}, and therefore offers a fascinating platform to study how long- and short-range polar orders coexist and compete²¹.

Diffuse scattering measurements are very sensitive to inhomogeneities in various materials systems, and have been used extensively to probe the SRPO in relaxors²²⁻³³. In general we find that in lead-based relaxors such as PMN-*x*PT and their analogue PZN-*x*PT, the diffuse scattering is dominated by intensities extending along $\langle 110 \rangle$ directions in reciprocal space (see Fig. 1), which is sometimes denoted as the "butter-fly diffuse" [due to its shape in the (HK0) scattering plane] or "T2 diffuse" (due to its relation to T2 phonon modes in the system)³⁴. In order to determine how the SRPO affect ferroelec-

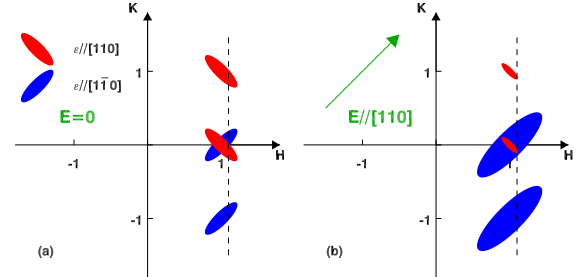


FIG. 1. Schematic of the diffuse scattering intensity distribution in the (HK0) plane under (a) zero field, and (b) a E-field along [110] direction. The red and blue "wings" are intensities associated with mostly [110] and [1 $\bar{1}$ 0] polarizations, respectively. The dashed lines indicate the locations of the (1.1,0,K) linear scans described in the text.

tric properties of these materials, it would be of great interest to study the response of the diffuse scattering to external electric field along different directions. In this paper we discuss our results of neutron diffuse scattering measurements on a single crystal of PMN-28%PT under an external field along [110] direction.

The single crystal of PMN-28%PT is grown by a modified Bridgman method at Penn State University. It is located on the left side but very close to the MPB. In zero-field, the system undergoes a cubic-tetragonal-rhombohedral/monoclinic phase transition upon cooling, with $T_{C1} \sim 440$ K and $T_{C2} \sim 390$ K. The neutron diffuse scattering measurements have been carried out on SPINS cold triple-axis-spectrometer at the NCTR, with fixed $E_F=5.0$ meV, and collimations of Guide-80-80-open. Be filters are used both before and after the sam-

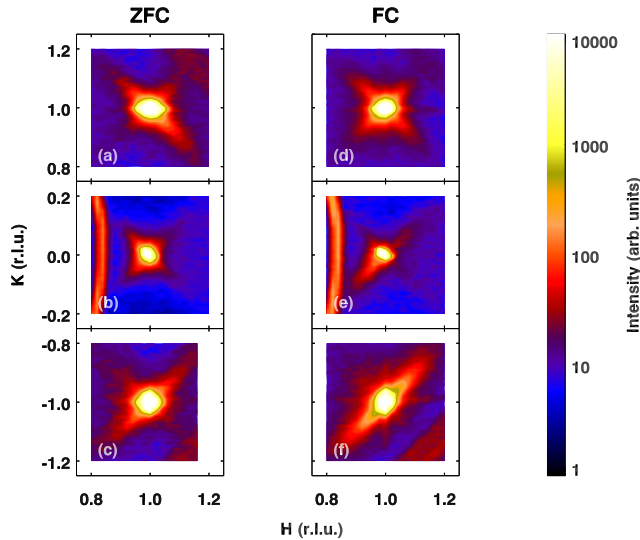


FIG. 2. Mesh intensity maps measured at 300 K in the (HK0) plane near (110) (top row), (100) (center row) and $(1\bar{1}0)$ (bottom row) Bragg peaks. The left column shows intensities measured under ZFC, while the right column shows measurements under FC of $E=1$ kV/cm along [110].

ple to reduce higher order neutrons. Measurements have been performed in both the (HK0) and (HOL) planes while the external electric field is applied along the [110] direction.

The diffuse scattering intensity distributions under ZFC measured at 300 K are shown in the left column of Fig. 2. They are consistent with the known behavior of the T2-diffuse in PMN/PZN type relaxors where the intensity has a butterfly shape near (100) and are elongated along the transverse directions near (110) and $(1\bar{1}0)$ Bragg peaks. The diffuse scattering intensity from the SRPO is a result of displacement type (short-range) order and follows the $|\mathbf{Q} \cdot \epsilon|^2$ factor where \mathbf{Q} is the wave-vector transfer and ϵ is the polarization vector (atomic shift). If one decomposes the T2-diffuse in the (HK0) plane into two "wings" (red and blue, shown in Fig. 1), it would be reasonable to associate the red "wing" with [110] type local polarizations, based on its being intense around $\mathbf{Q} = (110)$ and weak/absent around $\mathbf{Q} = (1\bar{1}0)$. Likewise, the blue "wing" intensity is naturally associated with $[1\bar{1}0]$ type polarizations³³. Under ZFC, in average these wings are equally intense near the (100) Bragg peak.

A linear intensity profile taken along $[1.1, K, 0]$ (the dashed line in Fig. 1) can be used to monitor how these two "wings" change without having to complete the entire 2D intensity mesh. In the left column of Fig. 3, we show the temperature dependence of the diffuse scattering intensity along $[1.1, K, 0]$ upon ZFC. Because this dashed line is taken on the right side (positive H side) of all three [(110), (100) and $(1\bar{1}0)$] Bragg peaks, the red wing intensity is always going to show up on the left side (negative K side) of the blue wing intensity. From the data one can clearly see that the diffuse scattering intensity grows upon cooling - the growth is more pronounced near

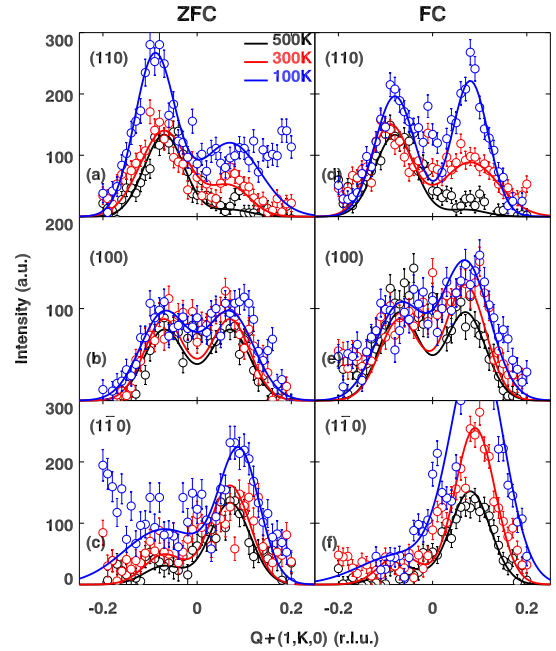


FIG. 3. Linear intensity profiles measured along $[1.1, K, 0]$ at 100 K (blue), 300 K (red) and 500 K (black). The left column shows intensities measured under ZFC, while the right column shows measurements under FC of $E=1$ kV/cm along [110].

(110) and $(1\bar{1}0)$ than (100) suggesting a change of the diffuse scattering structure factors across different Bragg peaks upon cooling. As expected, the blue and red wing intensities develop equally near (100). Near (110), the red wing (the left peak) is much stronger, and near $(1\bar{1}0)$ the blue wing (the right peak) is dominating instead.

When an external field of $E=1$ kV/cm along [110] is applied at 500 K, mesh scans performed at 300 K [Fig. 2(d), (e) and (f)] indicate that intensities from the blue wing ($\epsilon_{blue}/[1\bar{1}0]$) are enhanced by the field and those from the red wing ($\epsilon_{red}/[110]$) are reduced. This is also apparent when we investigate the linear intensity profiles along $[1.1, K, 0]$ (Fig. 3), where the peak on the right side is significantly enhanced with FC. It is worth noting that the enhanced blue wing intensity is present even near the (110) Bragg peak, where \mathbf{Q} is perpendicular to ϵ_{blue} . There could be two possible explanations, (i) the polarization of the SRPO that contribute to the blue wing intensity could have been slightly affected by the field and therefore not entirely perpendicular to \mathbf{Q} anymore; or (ii) these SRPO are dominated by $\langle 110 \rangle$ type polarizations, but could still have a small portion of polarization components along other directions, and therefore the blue wing intensity is never completely extinct near (110). The latter seems more plausible since that even without an external field, small traces of the blue wing intensities can still be observed near (110) [see Fig. 1(a) and (c), also small traces of red wing intensities near $(1\bar{1}0)$].

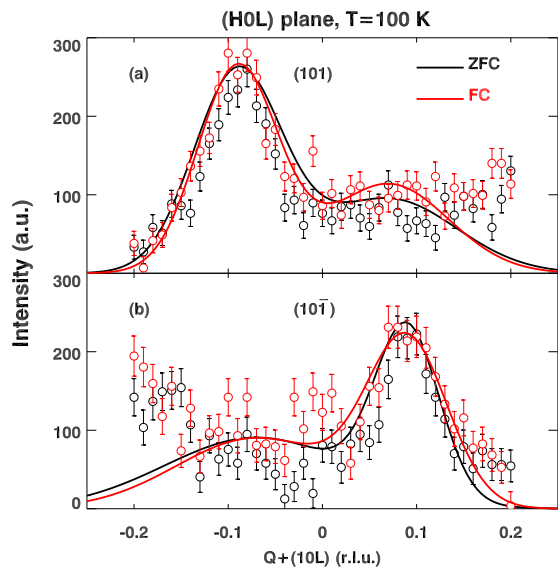


FIG. 4. Linear intensity profiles measured along $[1.1,0,L]$ at 100 K near (101) and $(10\bar{1})$. ZFC measurements are shown in black, while FC ($E=1\text{kV/cm}$ along $[110]$) measurements are shown in red.

While in the $(HK0)$ plane we observe this $[110]$ -field induced redistribution of diffuse scattering intensity from SRPO with $\epsilon_{red} // [110]$ to $\epsilon_{blue} // [1\bar{1}0]$ in the low temperature phase, it is important to perform similar measurements on diffuse scattering in $(H0L)$ and/or $(0KL)$ planes. Our findings are that the diffuse scattering intensities in the low temperature R-phase are not affected by the $[110]$ field in these planes. An example of intensity profiles along $[1.1,0,L]$ (in $(H0L)$ plane) are shown in Fig. 4. The field has no effect for diffuse scattering intensities near either the (101) or $(10\bar{1})$ Bragg peaks. Suggesting that the $[110]$ field does not affect diffuse scattering intensities from SRPO with ϵ along $[101], [10\bar{1}]$ [measured in $(H0L)$ plane], $[011]$, and $[01\bar{1}]$ [measured in $(0KL)$ plane].

In Table I we summarize the observed electric field effect on various T2-diffuse components associated with different $\langle 110 \rangle$ polarizations. We find that the results are not sensitive to the strength of the field (moderate E-fields ranging from 0.5 kV/cm to 4 kV/cm all have similar effect). We also include results of $[001]$ and $[111]$ field reported in previous work^{20,33,35} for comparison. We notice that in general, one sees a trend that when the polarization of the SRO is perpendicular to the field, the associated diffuse scattering component is likely to be enhanced (e.g. the case of $\epsilon // [1\bar{1}0]$ and $E // [110]$, or $\epsilon // [1\bar{1}0]$ and $E // [111]$, etc.). This is however, not always the case, for example, for $E // [001]$, even when $\epsilon // [110]$ which is perpendicular to E , no enhancement occurs.

These types of field effects on T2-diffuse scattering are never observed for temperatures greater than T_C . In addition to the FC measurements, they can also be induced directly at low temperature by applying a field to the sample without having to go through a field cooling process through T_C . Moreover, these effects persist at low temperature even after the field is removed. This type of history dependence

TABLE I. Electric field induced intensity change of diffuse scattering associated with short-range polarizations with ϵ along different $\langle 110 \rangle$ directions. "NC" denotes "no change".

ϵ	$[110]$	$[1\bar{1}0]$	$[101]$	$[10\bar{1}]$	$[011]$	$[01\bar{1}]$
$E // [110]$	-	+	NC	NC	NC	NC
$E // [111]$	-	+	-	+	-	+
$E // [001]$	NC	NC	NC	NC	NC	NC

suggests a connection to the formation of ferroelectric domains. Being on the left side of the MPB, the low temperature ground state of PMN-28%PT (and other PZN- x %PT and PMN- x %PT solid solutions with low PT concentrations) is in average rhombohedral, or, upon FC, monoclinic, that are slightly modified from the rhombohedral state. Therefore the polarizations of the ferroelectric domains are $\langle 111 \rangle$ (R-phase) or slightly rotated from $\langle 111 \rangle$ (M-phases).

The observed change of T2 diffuse scattering intensity distribution can only be explained if, within each of the $\langle 111 \rangle$ ferroelectric domains, local regions with different $\langle 110 \rangle$ SRPO are not equally populated. Consider the case of E-field along $[111]$, the configuration in Table II would be a natural solution. Here we propose that in ferroelectric domains with the four different $\langle 111 \rangle$ type polarizations (we ignore the positive/negative polarity), only local regions with SRPO perpendicular to the surrounding polarization can develop. If an external field along $[111]$ is applied which can increase the volume of P_{111} , consequently, diffuse scattering intensities associated with $[1\bar{1}0], [10\bar{1}]$, and $[01\bar{1}]$ local polarizations are enhanced²⁰ (see Table I too). In the case of an external field along $[001]$ direction, the field effect on the four domains (P_{111} , $P_{1\bar{1}\bar{1}}$, $P_{\bar{1}11}$, and $P_{\bar{1}\bar{1}1}$) are the same and none of these is more favored than the other. Therefore one will not observe any clear change of the T2-diffuse scattering intensity distribution.

In the current case, when a $[110]$ field is applied, the situation is a bit more complicated. One would expect the $P_{1\bar{1}\bar{1}}$ and $P_{\bar{1}\bar{1}1}$ domains to diminish since they have polarizations perpendicular to the field and are not favored in energy during the domain formation process. The other two domains, P_{111} and $P_{11\bar{1}}$ would have increased volumes (compared to the zero-field condition). The polarizations of these domains can of course, be rotated away slightly from the $[111]$ and $[11\bar{1}]$ directions in the corresponding monoclinic planes by the field, which nevertheless, does not affect our discussion for the SRPO. As a result, based on our proposed SRPO distribution in different ferroelectric domains in Table II, volume of SRPO along $[1\bar{1}0]$ will increase (present in both P_{111} and $P_{11\bar{1}}$), and that of SRPO along $[110]$ will decrease (not present in either P_{111} or $P_{11\bar{1}}$). The volume of SRPO along $[101], [10\bar{1}], [011]$, and $[01\bar{1}]$ will not change (the volume increase from P_{111} and $P_{11\bar{1}}$ and the volume decrease from $P_{1\bar{1}\bar{1}}$ and $P_{\bar{1}\bar{1}1}$ cancel each other out for these SRPO). This naturally explains the partial redistribution of diffuse scattering intensities observed in this study (Table I).

The current results, when interpreted using this proposed picture, suggests that a moderate electric field mainly change

TABLE II. The distribution of short-range polarizations with ϵ along $\langle 110 \rangle$ directions in ferroelectric domains with different $\langle 111 \rangle$ polarizations. "Y" and "N" denote whether such a SRPO can develop in the ferroelectric domain.

ϵ	[110]	[$\bar{1}\bar{1}0$]	[101]	[$10\bar{1}$]	[011]	[$0\bar{1}\bar{1}$]
P_{111}	N	Y	N	Y	N	Y
$P_{\bar{1}\bar{1}\bar{1}}$	N	Y	Y	N	Y	N
$P_{1\bar{1}\bar{1}}$	Y	N	N	Y	Y	N
$P_{\bar{1}11}$	Y	N	Y	N	N	Y

the volumes of various ferroelectric domains, rather than affecting the SRPO directly. This reiterates results from other work showing that the SRPO are strongly dependent on the chemical short-range order^{36,37}, where the latter is obviously not sensitive to a moderate electric field. In addition, our field-measurements provides a way to understand how the SRPO and long-range ferroelectric order coexist, by tuning the relative volumes of domains with different long-range polarizations. The configuration where the SRPO develop with polarizations perpendicular to that of their surrounding ferroelectric domains may at first appear aberrant since it is clearly not an energy-favorable state. We do not have a convincing explanation for why this configuration could occur. However, one may look at the problem from another perspective. The SRPO can be observed in these relaxor compounds, because they differ from the surrounding environment. If local SRPO develop with polarizations similar to the surrounding lattice matrix (in the low temperature ferroelectric phase), they may

eventually blend into the polar lattice and become hard to distinguish. On the other hand, local polarizations perpendicular to the surrounding lattice will always remain distinguishable and stand out in any bulk measurements that are sensitive to local polarizations that deviate from the lattice matrix.

Overall, we have shown that in PMN-28%PT, a partial redistribution of T2-diffuse scattering intensity can be induced by a moderate electric field applied along [110] direction in the low temperature (R) phase. Our results, together with previous results on the full-redistribution of T2-diffuse scattering intensities under [111] field, and the lack of change of the T2-diffuse scattering intensities under [001] field, can all be well accounted for if the SRPO in these relaxor compounds are distributed in a configuration where they develop mainly with $\langle 110 \rangle$ polarizations normal to the $\langle 111 \rangle$ -type polarizations in the surrounding R-type ferroelectric domains. More work on the SRPO in other phases, and theoretical considerations on why this configuration can be established in the first place, are clearly needed.

ACKNOWLEDGMENTS

FL acknowledges the National Natural Science Foundation of China (Grants No. 51572214) and the Key Science and Technology project of Shanxi Province (2018KJXX-081). SZ acknowledges the support of ONRG under Grant No. N62909-18-12168. CS acknowledges the Carnegie Trust for the Universities of Scotland and the Royal Society.

- ¹ S.-E. Park and T. R. Shrout, *J. Appl. Phys.* **82**, 1804 (1997).
- ² K. Uchino, *Piezoelectric actuators and ultrasonic motors* (Kluwer Academic, Boston, 1996).
- ³ R. F. Service, *Science* **275**, 1878 (1997).
- ⁴ S. Zhang and F. Li, *Journal of Applied Physics* **111**, 031301 (2012).
- ⁵ Y. Imry and S. Ma, *Phys. Rev. Lett.* **35**, 1399 (1975).
- ⁶ B. I. Halperin and C. M. Varma, *Phys. Rev. B* **14**, 4030 (1976).
- ⁷ V. Westphal, W. Kleemann, and M. D. Glinchuk, *Phys. Rev. Lett.* **68**, 847 (1992).
- ⁸ R. Fisch, *Phys. Rev. B* **67**, 094110 (2003).
- ⁹ R. Pirc and R. Blinc, *Phys. Rev. B* **60**, 13470 (1999).
- ¹⁰ G. Burns and F. H. Dacol, *Phys. Rev. B* **28**, 2527 (1983).
- ¹¹ L. E. Cross, *Ferroelectrics* **76**, 241 (1987).
- ¹² Z. Kutnjak, J. Petzelt, and R. Blinc, *Nature* **441**, 956 (2006).
- ¹³ F. Li, S. Zhang, T. Yang, Z. Xu, N. Zhang, G. Liu, J. Wang, J. Wang, Z. Cheng, Z.-G. Ye, J. Luo, T. R. Shrout, and L.-Q. Chen, *Nature Communications* **7**, 13807 (2016).
- ¹⁴ F. Li, S. Zhang, D. Damjanovic, L.-Q. Chen, and T. R. Shrout, *Phys. Rev. B* **28**, 1870262 (2018).
- ¹⁵ J.-M. Kiat, Y. Uesu, B. Dkhil, M. Matsuda, C. Malibert, and G. Calvarin, *Phys. Rev. B* **65**, 064106 (2002).
- ¹⁶ D. E. Cox, B. Noheda, G. Shirane, Y. Uesu, K. Fujishiro, and Y. Yamada, *Appl. Phys. Lett.* **79**, 400 (2001).
- ¹⁷ B. Noheda, D. E. Cox, G. Shirane, J. Gao, and Z.-G. Ye, *Phys. Rev. B* **66**, 054104 (2002).
- ¹⁸ C. Stock, D. Ellis, I. P. Swainson, G. Xu, H. Hiraka, Z. Zhong, H. Luo, X. Zhao, D. Viehland, R. J. Birgeneau, and G. Shirane, *Phys. Rev. B* **73**, 064107 (2006).
- ¹⁹ G. Xu, P. M. Gehring, and G. Shirane, *Phys. Rev. B* **72**, 214106 (2005).
- ²⁰ G. Xu, P. M. Gehring, and G. Shirane, *Phys. Rev. B* **74**, 104110 (2006).
- ²¹ Guangyong Xu, *J. Phys. Soc. Japan* **79**, 011011 (2010).
- ²² H. You and Q. M. Zhang, *Phys. Rev. Lett.* **79**, 3950 (1997).
- ²³ K. Hirota, Z.-G. Ye, S. Wakimoto, P. M. Gehring, and G. Shirane, *Phys. Rev. B* **65**, 104105 (2002).
- ²⁴ B. Dkhil, J. M. Kiat, G. Calvarin, G. Baldinozzi, S. B. Vakhrushev, and E. Suard, *Phys. Rev. B* **65**, 024104 (2001).
- ²⁵ S. N. Gvasaliya, S. G. Lushnikov, and B. Roessli, *Phys. Rev. B* **69**, 092105 (2004).
- ²⁶ D. La-Orauttapong, J. Toulouse, J. L. Robertson, and Z.-G. Ye, *Phys. Rev. B* **64**, 212101 (2001).
- ²⁷ D. La-Orauttapong, J. Toulouse, Z.-G. Ye, W. Chen, R. Erwin, and J. L. Robertson, *Phys. Rev. B* **67**, 134110 (2003).
- ²⁸ J. Hlinka, S. Kamba, J. Petzelt, J. Kulda, C. A. Randall, and S. J. Zhang, *J. Phys.: Condens. Matter* **15**, 4249 (2003).
- ²⁹ H. Hiraka, S.-H. Lee, P. M. Gehring, G. Xu, and G. Shirane, *Phys. Rev. B* **70**, 184105 (2004).
- ³⁰ G. Xu, G. Shirane, J. R. D. Copley, and P. M. Gehring, *Phys. Rev. B* **69**, 064112 (2004).
- ³¹ S. B. Vakhrushev, A. A. Naberezhnov, N. M. Okuneva, and B. N. Savenko, *Phys. Solid State* **40**, 1728 (1998).
- ³² M. Matsuura, K. Hirota, P. M. Gehring, Z.-G. Ye, W. Chen, and

- G. Shirane, Phys. Rev. B **74**, 144107 (2006).
- ³³ G. Xu, Z. Zhong, H. Hiraka, and G. Shirane, Phys. Rev. B **70**, 174109 (2004).
- ³⁴ Zhijun Xu, Jinsheng Wen, Guangyong Xu, C. Stock, J. S. Gardner, and P. M. Gehring, Phys. Rev. B **82**, 134124 (2010).
- ³⁵ Jinsheng Wen, Guangyong Xu, C. Stock, and P. M. Gehring, Appl. Phys. Lett. **93**, 082901 (2008).
- ³⁶ B. P. Burton, E. Cockayne, S. Tinte, and U. V. Waghmare, Phase Transitions **79**, 91 (2006).
- ³⁷ S. Prosandeev and L. Bellaiche, Physical Review B **94**, 180102(R) (2016).